ChemPubSoc Europe

DOI: 10.1002/chem.201xxxxxx

CHEMISTRY
A European Journal
Full Paper

Supramolecular Nanoscience

Shape-Persistent and Adaptive Multivalency – Rigid Transgeden (TGD) and Flexible PAMAM Dendrimers for Heparin Binding

Stephen M. Bromfield,[‡[a]] Paola Posocco,[‡[b]] Maurizio Fermeglia,[[b]] Juan Tolosa,[[c]] Ana Herreros-López,[[c]] Sabrina Pricl,*[[b]] Julián Rodríguez-López*[[c]] and David K. Smith*[[a]]

Abstract: This paper investigates Transgeden (TGD) dendrimers (polyamidoamine (PAMAM) type dendrimers modified with rigid polyphenylenevinylene (PPV) cores) and compares their heparin-binding ability with commercially available PAMAM dendrimers. Although the peripheral ligands are near-identical between the two dendrimer families, their heparin binding is very different. At low generation (G1), TGD outperforms PAMAM, but at higher generation (G2 and G3), the PAMAMs are better. Heparin binding also depends strongly on the dendrimer:heparin ratio. We explain these effects using multiscale modelling. TGD dendrimers exhibit 'shape-persistent multivalency' – the rigidity means that small clusters of surface amines are locally well optimised for target binding, but it prevents the overall nanoscale structure from rearranging to maximise its contacts with a single heparin chain. Conversely, PAMAM dendrimers exhibit 'adaptive multivalency' – the flexibility means individual surface ligands are not so well optimised locally to bind heparin chains, but the nanostructure can adapt more easily and maximise its binding contacts. As such, this paper exemplifies important new paradigms in multivalent biomolecular recognition.

Introduction

Multivalency has emerged as one of the most important ways in which nanoscale recognition can be achieved in competitive media.[1] Organising multiple ligands on the surface of a nanoscale architecture enhances binding as a consequence of entropic factors and an increase in local concentration of ligand at the binding interface. Multivalent binding is of particular importance given that many biological objects, from cell membranes to proteins and nucleic acids, have nanoscale dimensions. In recent times chemists have increasingly focussed on ways in which multivalent ligand arrays can be arranged to maximise binding.

Dendrimers are well-defined molecules with repeating branched motifs, which therefore have multiple functional groups on their surfaces.[2] As such, they constitiute one of the best ways of organising a multivalent ligand array. Some of the simplest and best-known dendrimers exhibit multivalent binding to well-known biological targets – for example, poly(amidoamine) (PAMAM) dendrimers are used for DNA binding and gene delivery, with the polycationic surface amines of PAMAMs binding via multivalent electrostatic interactions and hydrogen bonding to the anionic phosphates on DNA.[3] A number of reports have investigated the effect of dendritic size (generation) on binding – for example it is known that for effective gene delivery, higher generation dendrimers are more effective as not only do they bind DNA in a more multivalent manner, but the 'spare' internal tertiary amines can buffer the interior of endosomes and assist endosomal escape – a key step in gene delivery.[4] PAMAM dendrimers have also been used to bind and deliver siRNA.[5]

The ability of PAMAMs to achieve multivalent binding with other biomolecules has also been studied. For example, heparin, an anionic polysaccharide, plays a key role as anti-coagulant during major surgery, and there has been considerable interest in developing heparin sensors[6] and binders[7] which have potential medicinal use either for quantifying heparin in the bloodstream or reversing the effect of heparin once surgery is complete.[8] There have been several reports in which the interaction between PAMAM dendrimers and heparin has been quantified.[9] In recent work, we established a new heparin binding dye-displacement assay to demonstrate that intermediate sized PAMAM dendrimers (G2 to G4) gave the most effective binding in terms of charge efficiency.[10] Smaller G1 dendrimers were not sufficiently

[a] Prof. D. K. Smith and Mr S. M. Bromfield
Department of Chemistry
University of York
Heslington, York, YO10 5DD, UK
Fax: (+44) 1904 324516
E-mail: david.smith@york.ac.uk

[b] Prof. S. Pricl, Prof. M. Fermeglia, Dr P. Posocco
Simulation Engineering (MOSE) Laboratory, Department of Engineering and Architecture (DEA),
University of Trieste
34127, Trieste, Italy
E-mail: sabrina.pricl@di3.units.it

[c] Prof. J. Rodríguez-López, Dr. J. Tolosa, Ms A. Herreros-López
Área de Química Orgánica, Facultad de Ciencias y Tecnologías Químicas,
Universidad de Castilla la Mancha
13071 Ciudad Real, Spain
E-mail: Julian.Rodriguez@uclm.es

Supporting information for this article is available on the WWW under http://www.chemeurj.org/ or from the author.

multivalent to bind heparin effectively, while larger G6 dendrimers were unable to marshal all of their charges in heparin binding, and a significant number of them were therefore 'wasted'.

There has been much interest in modified PAMAM structures for gene binding and delivery. For example, more flexible PAMAM derivatives are highly effective.[11] PAMAM dendrons have also been attached to flexible cores and used for DNA binding.[12] Self-assembly of amphiphilic PAMAM dendrons into supramolecular dendrimers can enhance multivalent binding and biological activity.[13] More rigid analogues of PAMAMs have also been reported – for example the Transgeden dendrimers (TGDs, Figure 1).[14] TGD dendrimers have conjugated photoactive poly(phenylene vinylene) (PPV) cores, with peripheral PAMAM-like groups, and exhibit effective siRNA binding, delivery into neuronal cells, and also have useful optical properties.

In this new paper, we wanted to explore the binding of TGDs to heparin. We reasoned that using our recently developed Mallard Blue dye-displacement assay,[10] we should be able to quantify the performance of TGD and compare the data to the original PAMAM dendrimers. We hoped this would provide insight into the nature of the multivalent ligand display which can be achieved on different types of dendrimer scaffold – flexible vs rigid. Other authors have explored dendrons for DNA binding and referred to them as flexible and/or rigid – however, the structures were all relatively flexible and differences were limited. [15]

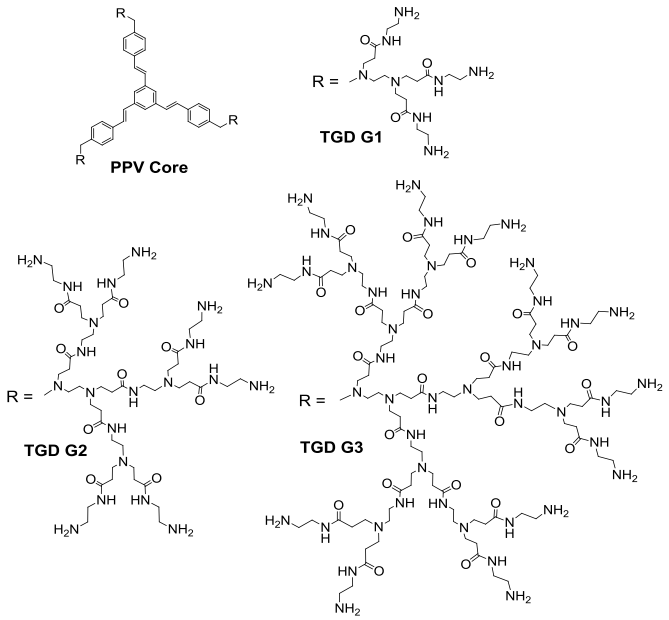

Figure 1. Structures of PPV core and associated PAMAM surface groups for first (TGD-G1), second (TGD-G2) and third (TGD-G3) generation Transgeden hybrid dendrimers.

Results and Discussion

Experimental Study of Heparin Binding Using Mallard Blue Displacement Assay

To study the binding of TGD dendrimers (Fig. 1) to heparin we employed our previously published Mallard Blue (MalB) indicator displacement assay conditions,[10] in which a solution of dendrimer was titrated into a cuvette containing MalB and heparin before measuring the absorbance of the resulting solution. All concentrations, except that of the binder under test, were kept constant throughout the assay: MalB (25 μM), heparin (27 μM), NaCl (150 mM), Tris HCl (10 mM, pH 7.0). Binding data are presented in terms of the effective concentration required to displace half of the MalB (EC_{50}) from heparin, the charge excess of cationic binder at this point (CE_{50}, i.e., the cation/anion ratio, assuming that dendrimer surface amines are all charged, and heparin has a tetra-anionic disaccharide repeat unit) and the effective dose of the binder (in mg per 100 international units [IU] of heparin) (Table 1). As supplied, only ~30-40% of heparin chains have the active sequence of pentasaccharide repeat units which confer high anti-coagulant activity. However, all of the material contains anionic saccharides, even if not active, which will be bound. The heparin concentration in this paper refers to the total concentration of anionic disaccharide, irrespective of whether it is in the active form or not, and this value is used to calculate the CE_{50} and EC_{50} values. For calculating the 'dose', however, we reference the activity of the heparin binder only to the clinically active heparin (in IU). It should also be noted that, as documented in the literature, this type of dendrimer is acutely sensitive to pH.[16] In our assay (pH 7.0), only the primary amines at the dendrimer surface are protonated and only these charges are counted in calculation of CE_{50} values.

Table 1. Heparin binding data for Transgeden (TGD) and Poly(amidoamine) (PAMAM) dendrimers

Compound	Surface Charge	EC_{50} [μM][a]	CE_{50}[b]	Dose[c] [mg/100IU]
TGD-G1	+9	7.73 ± 0.32	0.64 ± 0.03	0.38 ± 0.02
TGD-G2	+18	3.78 ± 0.25	0.63 ± 0.04	0.42 ± 0.03
TGD-G3	+36	2.00 ± 0.15	0.67 ± 0.05	0.47 ± 0.04
PAMAM-G1	+8	10.10 ± 0.32	0.75 ± 0.02	0.44 ± 0.01
PAMAM-G2	+16	2.55 ± 0.32	0.38 ± 0.04	0.25 ± 0.03
PAMAM-G3	+32	1.53 ± 0.21	0.45 ± 0.06	0.32 ± 0.04

[a] EC_{50} is effective concentration of dendrimer for 50% displacement for MalB (25 μM) from heparin (27 μM tetra-anionic disaccharide). [b] CE_{50} is the charge excess (cation:anion) required for 50% displacement of MalB. [c] Dose is the mass of dendrimer required to bind 100IU of heparin.

From the data in Table 1, it can be seen that all generations can bind heparin and displace MalB. The higher generation TGDs operate at lower concentrations (i.e. EC_{50} decreases) – this reflects the larger number of amines on their surfaces (see below). Interestingly, however, in charge efficiency terms, all three generations of TGD have very similar CE_{50} values for binding heparin. Comparing the CE_{50} values of the TGD dendrimers therefore suggests that the larger dendrimers do not become more efficient on a per charge basis. In terms of dose (by weight), the smallest dendrimer, with the lowest molecular mass, is actually the best heparin binder.

These data are somewhat surprising, particularly if directly compared to the previously studied PAMAM dendrimers (Table 1). At low generation, TGD-G1 is more effective than PAMAM-G1 in terms of heparin binding. In previous work, it was also found that TGD-G1 was the optimal system for gene delivery, combining good efficacy with low toxicity.[14] However, at larger second and third generations, PAMAM dendrimers significantly improve their

performance while the TGD dendrimers do not. As such PAMAM-G2 is the most effective heparin binder in terms of CE_{50} by some margin over any of the TGD analogues. The inferior performance of TGD with respect to native PAMAMs clearly suggests that the presence of the PPV core somehow alters the effectiveness of each charge at the dendrimer surface when binding heparin. We proposed that the rigid core may somewhat restrict the ability of the charges to cooperate as effectively as in unmodified PAMAMs, possibly by preventing the reorganisation of surface ligands (see modelling below for detailed discussion) – we have previously reflected on the benefits of flexibility in multivalent arrays applied in DNA binding.[17]

Importantly, however, it should be noted that consideration of only the CE_{50} values as described above significantly limits the information which can be extracted from the assay as it only focusses on the dendrimer performance when half of the MalB is displaced from its complex with heparin – this corresponds to just one specific molar ratio of dendrimer:heparin. The performance of dendrimers may of course vary with molar ratio, depending on the stoichiometries of the complexes which can be formed. As such, it is worth looking at data from across the whole range of concentrations in a comparative sense.

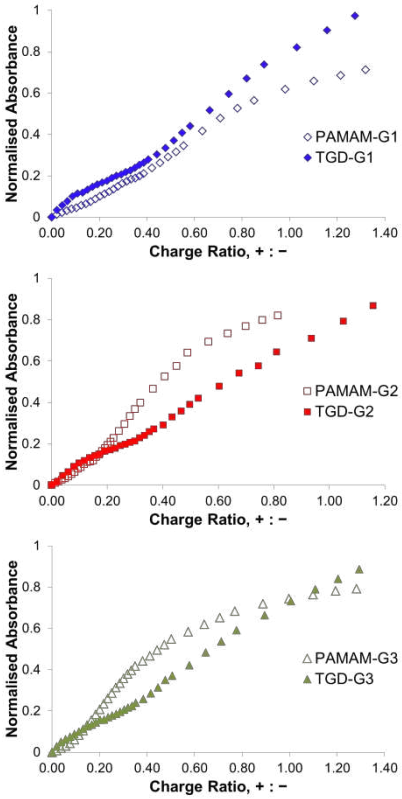

Figure 2. Titration of TGD and PAMAM dendrimers to displace MalB from its complex with heparin. Top, TGD-G1 and PAMAM-G1; Centre, TGD-G2 and PAMAM-G2; Bottom, TGD-G3 and PAMAM-G3.

Comparing low generation TGD-G1 and PAMAM-G1 (Fig. 2), it is clear that TGD outperforms PAMAM across the whole assay. As such, the CE_{50} value is a fair reflection of the overall data. Conversely, when comparing TGD-G2 and PAMAM-G2, or TGD-G3 and PAMAM-G3 (Fig. 2), when small amounts of TGD are present, TGD performs slightly better than PAMAM. However, as more dendrimer is added, the performance of TGD drops off, at which point PAMAM performs much better, and hence the CE_{50} values for PAMAM-G2 and PAMAM-G3, which sample just a single point of each experiment, appear much better than those for TGD-G2 and TGD-G3.

We propose that at low levels of dendrimer, the surface of the dendrimer will be saturated with binding interactions to multiple heparin chains – and we suggest that for TGD these interactions are quite well organised and strong. However, as the amount of TGD increases, there is less available heparin and each dendrimer will increasingly be forced to form interactions with just a single heparin chain – we suggest that TGD is less able to do this than PAMAM, perhaps as a consequence of TGD having higher rigidity and an inability to rearrange its surface to achieve effective binding of all surface groups (see modelling below).

Importantly, these data clearly show that charge alone is not enough to act as a simple predictor of heparin binding – if it did, then PAMAM and TGD dendrimers should have very similar heparin binding performance. It is sometimes suggested that when using electrostatic ion-ion interactions to bind polyanions, only the total charge and/or charge density are important.[18] It is also sometimes stated that selectivity can be very hard to achieve in ion-ion binding for this reason. However, our data show that quite simple changes can have a dramatic impact on the use of charge in binding. As such we suggest that spatial organisation is vital in this binding event and that careful charge organisation is a viable strategy through which selective ion-ion interactions in highly competitive aqueous media can be achieved.

To understand these experimental binding data, we decided to employ multiscale modelling in order to better answer the following questions:

(i) Why does TGD-G1 perform better than PAMAM-G1?

(ii) Why do PAMAM-G2 and G3 perform better than TGD-G2 and G3 at the CE_{50} value when more dendrimer is present?

(iii) Why do TGD-G2 and TGD-G3 appear to bind effectively to heparin when present in small amounts?

(iv) Why is the charge ratio-dependent behaviour different to that observed for PAMAM?

We reasoned that answering these questions would yield a detailed insight into multivalency effects and might help us understand the impact of rigid/flexible interiors on the behaviour of dendritic surface groups.

Theoretical Study of Heparin Binding Using Multiscale Modelling Methods[19]

i) Atomistic Molecular Dynamics Modeling at Charge Excess (CE) of 0.4

We started our modelling study by considering the performance of the dendrimers close to the CE_{50} value, at a consistent charge excess of 0.4 (cation:anion) using an atomistic molecular dynamics (MD)[20] approach. We used on a heparin chain with tetra-anionic disaccharide repeat units and the number of binding dendrimers was adjusted appropriately to give the required charge ratio of 0.4.

Table 2. Binding parameters from MD simulations at a charge excess of 0.4.

Compound	N_{mol}[a]	Q_{tot}[b]	Q_{eff}[c]	ΔG_{bind}^{eff} (kcal/mol)[d]	$\Delta G_{bind}^{eff}/Q_{tot}$ (kcal/mol)[e]	$\Delta G_{bind}^{eff}/Q_{eff}$ (kcal/mol)[f]
TGD-G1	4	36	26 ± 2	-9.6 ± 0.8	-0.27 ± 0.02	-0.37 ± 0.03
TGD-G2	2	36	21 ± 1	-9.9 ± 0.6	-0.28 ± 0.02	-0.47 ± 0.03
TGD-G3	1	36	14 ± 1	-10.1 ± 0.7	-0.28 ± 0.02	-0.72 ± 0.05
PAMAM-G1	5	40	35 ± 2	-10.2 ± 1.1	-0.26 ± 0.03	-0.29 ± 0.03
PAMAM-G2	2	32	29 ± 1	-44.7 ± 2.0	-1.40 ± 0.06	-1.54 ± 0.07
PAMAM-G3	1	32	15 ± 1	-15.9 ± 1.1	-0.50 ± 0.03	-1.06 ± 0.07

[a] N_{mol} is the number of dendrimer molecules included in the model. [b] Q_{tot} is the total positive charge associated with the dendrimers. [c] Q_{eff} is the number of positively charged amines on the dendrimers making effective binding contacts with heparin. [d] ΔG_{bind}^{eff} is the total effective free energy of binding between the dendrimers and heparin. [e] $\Delta G_{bind}^{eff}/Q_{tot}$ relates to the experimental CE_{50} value and indicates how well the total charge of the dendrimer is used in binding heparin. [f] $\Delta G_{bind}^{eff}/Q_{eff}$ represents how effective each active contact is in binding to heparin.

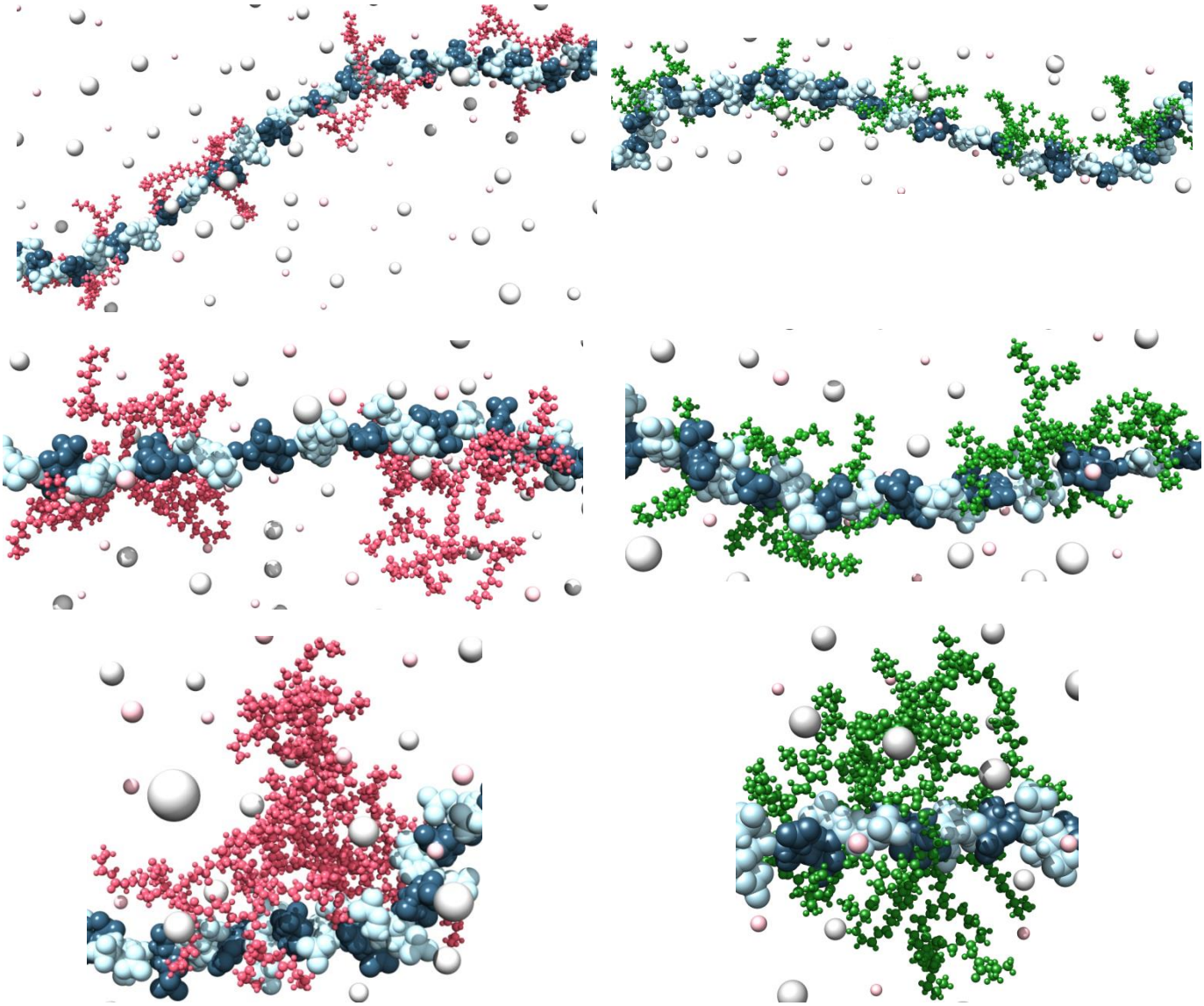

Figure 3. TGD-G1-G3 (left panels, top to bottom) and PAMAM-G1-G3 (right panels, top to bottom) dendrimers bound to heparin at a charge excess of 0.4 using MD modelling methods. TGD and PAMAM molecules are portrayed as pink and green sticks-and-balls, respectively. Heparin is shown as a chain of L-iduronic acid (blue) and D-glucosamine (light blue) alternating units. Some Na^+ and Cl^- counterions are shown as small and large pink and grey shaded spheres respectively. Water is not shown for clarity.

In the experimental data, at a charge excess of 0.4, PAMAM-G2 and PAMAM-G3 significantly outperform the TGD analogues, while TGD-G1 performs slightly better than PAMAM-G1. At this charge ratio there is approximately one TGD-G3 or PAMAM-G3 molecule per heparin chain (as modelled), two TGD-G2 or PAMAM-G2 molecules and ca. four (or five) TGD-G1 (or PAMAM-G1) molecules. The total charge associated with all of the dendrimers in the simulation is Q_{tot}. Using MD methods, we then calculate the total effective binding energy ΔG_{bind}^{eff} of these dendrimers with heparin. We can then normalise this by dividing by the total dendrimer charge present in the simulation (Q_{tot}). This should relate to the experimentally observed charge excess values, which are also calculated based on the total charge of dendrimer surface groups. We can also calculate the number of effective surface charges (that is, the charged residues actively contributing to binding to the heparin chain, Q_{eff}) and work out the effective binding energy of each active/binding surface charge with heparin ($\Delta G_{bind}^{eff}/Q_{eff}$).

Considering the data (Table 2) confirms that under these conditions, PAMAM-G2 and PAMAM-G3 are indeed the most effective heparin binders – in good agreement with the experimental observations. Furthermore, in terms of how the total charge of the dendrimer is used, TGD-G1, TGD-G2 and TGD-G3 all appear to be identical ($\Delta G_{bind}^{eff}/Q_{tot}$ = ca. -0.28 $kcalmol^{-1}$) – reflecting the CE_{50} values measured experimentally. Notably, TGD-G1 is also better than, or comparable with, PAMAM-G1 on a 'per dendrimer', or 'per charge', basis – once again in agreement with the experimental observations.

To understand differences in binding more precisely, and explore multivalency effects, it can be instructive to consider the performance of each active individual charge directly involved in a binding interaction. Considering the TGD dendrimers, it is clear that as the dendrimer becomes larger, fewer of the surface charges can actually contact heparin. This reflects the rigidity of the dendrimers, making it impossible for the surface charges to rearrange enough to bind to the heparin. For TGD-G1, 72% of the surface charges actively bind to heparin; this drops to 58% for TGD-G2 and 39% for TGD-G3. For the larger TGD dendrimers, those surface charges which do bind however, do so more effectively (as reflected in the effective binding energy of each active/binding surface charge, $\Delta G_{bind}^{eff}/Q_{eff}$) – but this only just manages to counterbalance the decrease in the number of such interactions – so the overall charge efficiency across all charges ($\Delta G_{bind}^{eff}/Q_{tot}$) remains constant. Figure 3 shows a snapshot of the modelling of heparin binding, indicating how a significant number of the surface charges for TGD-G2 and TGD-G3 simply cannot make contact with heparin. It appears that localised clusters of amines on the TGD surfaces appear to make contact – and we suggest that these are well-organised locally to bind heparin.

For the PAMAM dendrimers, the behaviour is significantly different – this is largely a consequence of the greater flexibility of the PAMAM structures. For PAMAM-G1, 87.5% of the available surface charges make good contact with heparin, and for PAMAM-G2 and PAMAM-G3 this value is 91% and 47%, respectively. These values are much larger than for TGD and reflect the flexible interior of PAMAM allowing significant reorganisation of the surface groups so that many more of them can interact with heparin. This can clearly be visualised in Figure 3 in which the PAMAM dendrimers rearrange and wrap their surface charges around the heparin polymer chain as best they can. We define this process as 'adaptive multivalency' – similar ability of flexible binding arrays to adapt at a binding interface have been previously noted.[17,21]

Comparing PAMAM-G1 with TGD-G1, it is clear that although the greater rigidity of TGD-G1 limits the number of surface charges which make contact with a single heparin chain, each individual active contact is more effective than for PAMAM-G1 (-0.37 kcal/mol vs -0.29 kcal/mol). This suggests that the cationic surface groups of rigid TGD-G1 are better pre-organised to bind heparin – but that once some of them have bound to the heparin chain, the molecule does not possess enough flexibility for the others to also come into contact with it (Fig. 3). It can be considered on structural grounds (Fig. 1) that TGD-G1 contains three separate groups of surface amines, each containing three locally pre-organised positive charges. Conversely, PAMAM-G1 does not locally organise small groups of amine, but its flexibility means that it can bring more of its weaker interactions to bear on the overall binding event across the whole dendrimer.

ii) Mesoscale Dissipative Particle Dynamics Modeling at CE 0.1

We then wanted to probe in more detail what happens at lower charge excess in the binding experiment (i.e. when a greater excess of heparin is present relative to dendrimer). Under these conditions, all of the TGD dendrimers appear experimentally, to perform somewhat better relative to PAMAM. We therefore performed mesoscale simulations using Dissipative Particle Dynamics (DPD)[22] at a charge excess of 0.1 (cation:anion) – this situation was ideal for mesoscale modelling as a consequence of the presence of multiple heparin chains and complex stoichiometries. Under these conditions, there is significantly more heparin relative to the dendrimers than in the MD modelling described above, and multiple heparin chains are now able to make contact with a single dendrimer. Obviously, in this case, the flexibility of the dendrimer, and the ability of multiple surface groups to make contact with a single heparin chain through adaptive multivalency, as described above, should become less relevant.

Figure 4 illustrates the binding of TGD-G1-G3 (top) and PAMAM-G1-G3 (bottom) to heparin. For the G1 systems, the heparin-dendrimer interactions are well-defined, with the geometry and conformation of TGD-G1 playing a key role in the binding process – more so than for PAMAM-G1 – we suggest this is a result of the greater rigidity of TGD providing local organisation of the surface ligands. As the generation of TGD increases, binding becomes less well-defined, with multiple heparins contacting one dendrimer. The stoichiometry of DNA binding has previously been considered in a similar way for PEI dendrimers.[23] The stoichiometry can be qualitatively appreciated by comparing the left and right panels of Figure 4; in the case of G1, mostly 1:1 dendrimer/heparin assemblies prevail (left-most panel) while for G3, several heparin chains contact a single dendrimer. This stoichiometry allows the formation of significantly more high affinity interactions for TGD than are present at higher charge excesses when less heparin is available. TGD suffered at a higher charge excess from not being able to use all of the rigidly displayed surface charges – conversely at lower charge excess they can now contact different parts of their well-optimised structure to different heparin chains significantly assisting binding.

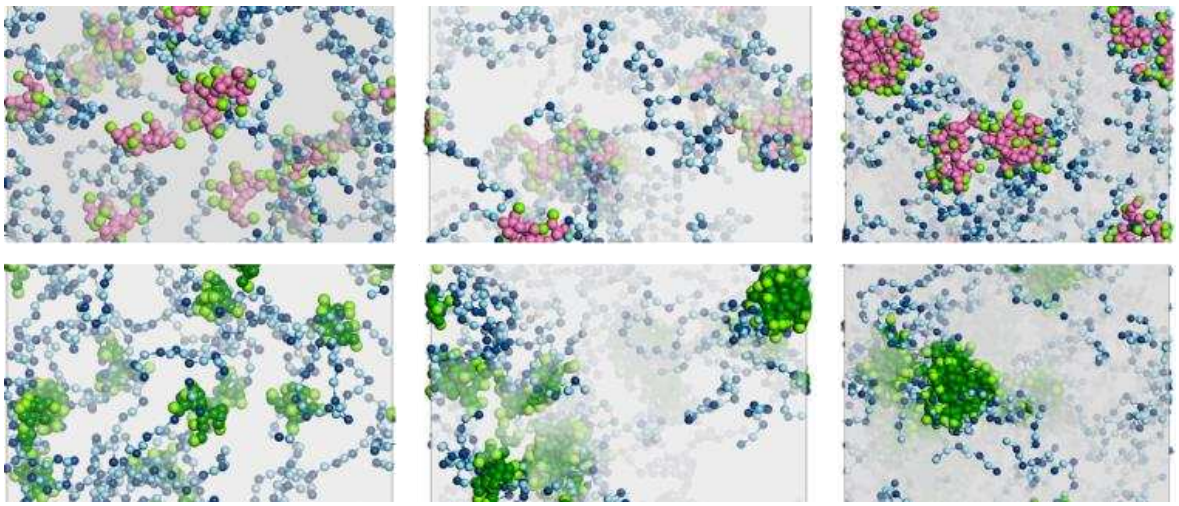

Figure 4. Zoomed view of the mesoscopic simulation of TGD and PAMAM dendrimers in complex with heparin at a charge excess of 0.1. Top (left to right) = TGD-G1, TGD-G2 and TGD-G3 binding to heparin. Bottom (left to right) = PAMAM-G1, PAMAM-G2 and PAMAM-G3 binding to heparin. PAMAM and TGD dendrimers are portrayed as green and pink spheres, respectively. Charged amine groups are depicted in light green for both families. Heparin is shown as a chain of L-iduronic acid (blue) and D-glucosamine (light blue) alternating units. A transparent grey field is used to represent water and ions.

We define this as 'shape-persistent multivalency' and propose that this explains why TGD dendrimers appear to perform more effectively at low charge excess, but less effectively at high charge excess.

To summarise the modelling studies, and answer the questions opened up by the experimental investigation:

(i) The rigidity of TGD-G1 means the surface ligands are displayed in a more locally organised, shape-persistent manner for heparin binding than on PAMAM-G1

(ii) The greater flexibility of PAMAM-G2 and PAMAM-G3 allows them to display adaptive multivalency and bring more of their surface groups into contact with a single heparin chain than TGD-G2 or TGD-G3

(iii) At low charge excess, multiple heparins can make contact with different parts of the locally organised surface of TGD-G2 and TGD-G3, which means that their shape-persistent multivalent surface ligands can all contribute to binding – leading to an improvement in relative performance under these conditions

(iv) The flexibility of the PAMAM dendrimers means they are better able to adapt to different binding stoichiometries and perform reasonably well at both low and high charge excesses.

Investigation of Heparin Binding Using Modified TGDs

To gain further insight into the role of surface charge in heparin binding, we investigated a family of modified TGD-G1 dendrimers in which some (or all) of the surface amines have been replaced with alcohol groups (Fig. 5).[24] This was done in a statistical manner during synthesis, and the degree of amine functionalisation estimated using a Kaiser test. Table 3 lists these dendrimers along with their estimated surface charge (in brackets) and details of their heparin binding performance. These data clearly show that none of the modified TGD-G1 dendrimers bind heparin as efficiently as TGD-G1. It is perhaps most interesting that removal of less than 20% of the positive charges from the periphery of TGD-G1 to afford TGD-G1 (+7.4) reduces the efficiency of each charge in binding by more than half.

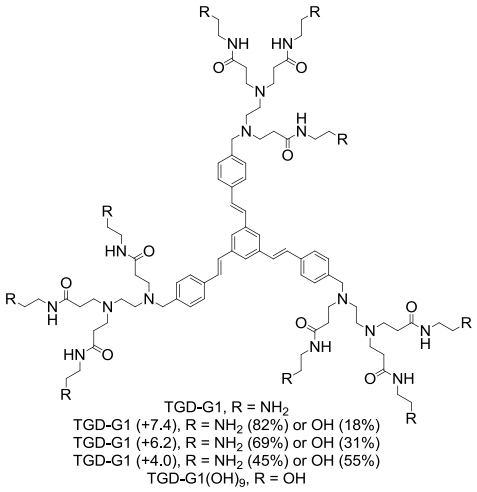

Figure 5. Structures of TGD-G1 with different levels of amine replacement by alcohol groups, including complete replacement (**TGD-G1(OH)$_9$**)

Table 3. Heparin binding data for Modified Transgeden (TGD) dendrimers

Compound	EC_{50} [μM][a]	CE_{50}[b]	Dose[c] [mg/100IU]
TGD-G1	7.73 ± 0.32	0.64 ± 0.03	0.38 ± 0.02
TGD-G1 (+7.4)	19.2 ± 2.7	1.31 ± 0.18	0.94 ± 0.13
TGD-G1 (+6.2)	*weak binding*	*weak binding*	*weak binding*
TGD-G1 (+4.0)	*weak binding*	*weak binding*	*weak binding*
TGD-G1$(OH)_9$	*no binding*	*no binding*	*no binding*

This suggests that all of the charged amines on the surface of the dendrimer are important, and that the absence of even a

few is significant. When even more amines are removed, the binding becomes very weak.

Table 4. Binding parameters from MD simulations at a charge excess of 0.4.

Compound	N_{mol}[a]	Q_{tot}[b]	Q_{eff}[c]	ΔG_{bind}^{eff} (kcal/mol)[d]	$\Delta G_{bind}^{eff}/Q_{tot}$ (kcal/mol)[e]	$\Delta G_{bind}^{eff}/Q_{eff}$ (kcal/mol)[f]
TGD-G1	4	36	26 ± 2	-9.6 ± 0.8	-0.27 ± 0.02	-0.37 ± 0.03
TGD-G1 (+7.4)	5	37	23 ± 1	-7.0 ± 0.4	-0.19 ± 0.01	-0.30 ± 0.02
TGD-G1 (+6.2)	6	37.2	23 ± 1	-4.9 ± 0.6	-0.13 ± 0.01	-0.21 ± 0.03

[a] N_{mol} is the number of dendrimer molecules included in the model. [b] Q_{tot} is the total positive charge associated with the dendrimers. [c] Q_{eff} is the number of positively charged amines on the dendrimers making effective binding contacts with heparin. [d] ΔG_{bind}^{eff} is the total effective free energy of binding between the dendrimers and heparin. [e] $\Delta G_{bind}^{eff}/Q_{tot}$ relates to the experimental CE_{50} value and indicates how well the total charge of the dendrimer is used in binding heparin. [f] $\Delta G_{bind}^{eff}/Q_{eff}$ represents how effective each active contact is in binding to heparin.

MD simulations of modified TGDs in the presence of heparin were performed at a charge excess of 0.4. As can be seen (Table 4), the binding decreases significantly on a per charge basis ($\Delta G_{bind}^{eff}/Q_{tot}$) – in agreement with the decrease observed experimentally in EC_{50} values. These data agree with a model in which the smaller parts of the rigid TGD dendrimer surface act fairly independently in terms of binding to heparin, with their rigidity limiting their ability to make the whole dendrimer surface cooperate. Given that TGD-G1 can be considered as containing three locally organised surface regions, each with three amines, we suggest statistically replacing just one of these three amines, has a significant negative impact on the binding of each surface group to heparin and hence considerably weakens binding.

Plotting the data in terms of charge excess (Fig. 6) provides an excellent example of multivalent charge organisation. By definition in this graph, there is the same total amount of positive charge present at each charge ratio, yet it is absolutely clear that TGD-G1 strongly outperforms the other dendrimers and has the best interactions with heparin as a consequence of its better locally organised multivalent binding surface.

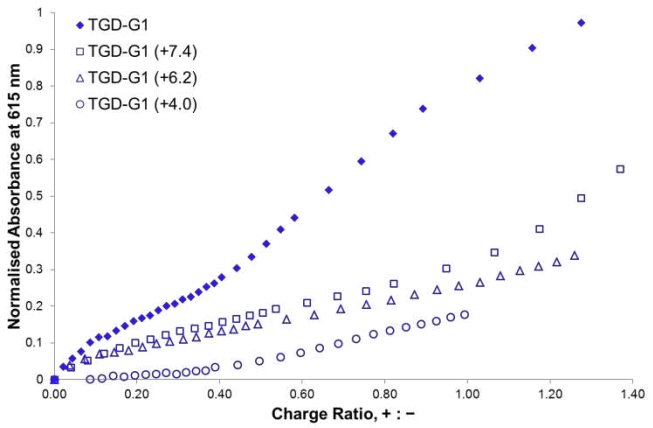

Figure 6. Binding curve comparison between TGD-G1, TGD-G1 (+7.4), TGD-G1 (+6.2), TGD-G1 (+4.0) and TGD-G1$(OH)_9$ expressed as a function of charge ratio.

Experimental Study of Heparin Binding Using the Inherent Fluorescence of TGD Dendrimers

Unlike PAMAM dendrimers, one key advantage of TGD dendrimers is that they have an inherent photophysically-active unit within their structure. As such, we can study heparin binding directly; in the absence of an indicator dye.

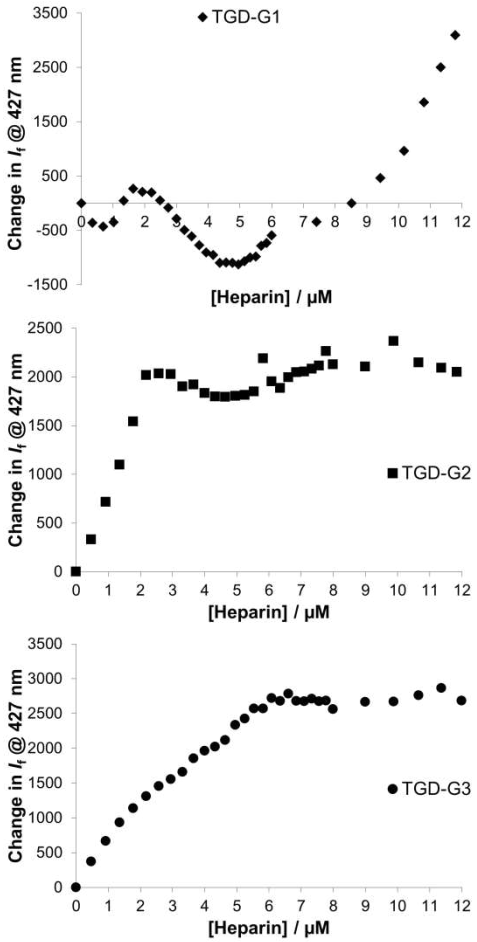

Figure 7. Plot of change in fluorescence intensity of a solution of dendrimer (1 μM) at 427 nm following irradiation at 318 nm against concentration of heparin: A, TGD-G1; B, TGD-G2; C, TGD-G3.

TGD-G1 has an absorbance maximum at 319 nm in water which, following irradiation, exhibits a complementary fluorescence output at 399 nm and 413 nm.[25] As such, a series of experiments was designed to titrate a solution of Transgeden (TGD-G1, TGD-G2 or TGD-G3) with heparin and monitor the spectroscopic response. Transgeden (1 μM) solutions were

made in aqueous solution in the presence of Tris-HCl buffer (10 mM, pH 7.0) and NaCl (150 mM). Plotting the resulting fluorescence intensity at λ_{max} (427 nm) against concentration of heparin yields the graphs in Figure 7.

For the larger dendrimers TGD-G2 and TGD-G3, conventional binding curves are observed, with an increase in fluorescence intensity on binding and saturation of fluorescence intensity. The higher generation dendrimer saturates at a larger heparin concentration, reflective of the greater number of heparin binding surface sites. The stoichiometry of the binding profiles would suggest saturation binding of two heparin disaccharide units (2 μM) to TGD-G2 and six (6 μM) to TGD-G3. This is in excellent agreement with the MD modelling illustrated in Figure 3 which indicates that this many disaccharide units can be covered by each dendrimer. The increase in fluorescence intensity may suggest that on binding, the core becomes more rigid, limiting non-radiative decay processes.[26] Conversely, TGD-G1 shows quite different behaviour, with some quenching of the fluorescence associated with the PPV core being initially observed before an increase in intensity. We suggest there may be some more direct interaction between bound heparin and fluorophore in this case meaning different effects are associated with different stoichiometries of complex (quenching versus rigidification), leading to the uninformative titration curve.

Nonetheless, it is clear that dendrimers TGD-G2 and TGD-G3 self-indicate heparin binding as a consequence of their optical properties, and act as heparin sensors. Clearly this role cannot be fulfilled by PAMAM dendrimers. There is a need for heparin sensors which can be used to detect heparin in plasma and given the large fluorescent response of TGD-G2 in competitive conditions of buffer and electrolyte, we suggest that this could be a candidate heparin sensor. 'Switch on' fluorescence sensing of this type is potentially useful in a clinical setting.[8]

Conclusion

In summary, we have demonstrated that TGD dendrimers appear, in general, to be less effective heparin binders than their PAMAM analogues. At low generation, TGD-G1 is better, but at higher generation, the PAMAM systems are better. However, the ability to bind also depends strongly on the ratio of dendrimer:heparin. In particular, in the presence of excess heparin, a clinically relevant situation, TGDs outperform PAMAMs. We can explain this in terms of the structure and dynamics of the dendrimer nanostructures as probed using multiscale modelling methods. We consider the TGD dendrimers to display shape-persistent multivalency, in which the rigidity means that small clusters/patches of surface amines are locally well-organised for target binding, but the overall nanoscale structure is not sufficiently flexible to maximise all of its contacts with a single heparin binding partner. PAMAM dendrimers conversely, exemplify adaptive multivalency, in which individual surface ligands are not so well locally optimised for target binding, but the flexibility of the overall nanostructure allows it to adapt its global shape more easily and hence maximise the total number and efficiency of contacts with the binding partner. Usefully, the rigid conjugated core of TGD dendrimers endows them with optical properties, and TGD-G2 and TGD-G3 can operate as 'switch-on' fluorescence sensors for heparin binding in competitive media.

Acknowledgements

SMB and DKS thank BBSRC and University of York for funding (DTA award) and COST Network TD0802 (Dendrimers in Biomedicine) for supporting networking within this project. Access to CINECA and supercomputing facility was granted to SP and PP through the sponsored HPC Italian Supercomputing Resource Allocation (ISCRA) projects SEA and DILUSO. JR-L thanks Ministerio de Ciencia e Innovación (Spain) / FEDER (EU) for financial support - project BFU2011-30161-C02-02.

Keywords: dendrimer • heparin • multiscale molecular modeling • molecular recognition • multivalency

1. (a) M. Mammen, S. K. Choi, G. M. Whitesides, *Angew. Chem. Int. Ed.* **1998**, *37*, 2755-2794. (b) A. Mulder, J. Huskens, D. N. Reinhoudt, *Org. Biomol. Chem.* **2004**, *2*, 3409-3424. (c) C. Fasting, C. A. Schalley, M. Weber, O. Seitz, S. Hecht, B. Koksch, J. Dernedde, C, Graf, E. W. Knapp, R. Haag, *Angew. Chem. Int. Ed.* **2012**, *51*, 10472-10498. (d) A. Barnard, D. K. Smith, *Angew. Chem. Int. Ed.* **2012**, *51*, 6572-6581.

2. (a) F. Vögtle, G. Richard, N. Werner, *Dendrimer Chemistry: Concepts, Syntheses, Properties, Applications*; Wiley-VCH: Weinheim, **2009**. (b) *Designing Dendrimers*; S. Campagna, P. Ceroni, F. Puntoriero, Eds.; Wiley: New York, **2011**. (c) *Dendrimers: Towards Catalytic, Material and Biomedical Uses*; A.-M. Caminade, C.-O. Turrin, R. Laurent, A. Ouali, B. Delavaux-Nicot, B., Eds.; Wiley: Chichester, **2011**.

3. For reviews and books see: (a) U. Boas, J. B. Christensen, P. M. H. Heegaard, *Dendrimers in Medicine and Biotechnology. New Molecular Tools*; RSC Publishing: Cambridge, **2006**. (b) *Dendrimer-Based Nanomedicine*; I. Majoros, J. R. Baker, Jr., Eds.; Pan Stanford Publishing: Singapore, **2008**. (c) M. A. Mintzer, E. E. Simanek, *Chem. Rev.* **2009**, *109*, 259-302. For key papers see: (d) J. Haensler, F. C. Szoka, *Bioconjugate Chem.* **1993**, *4*, 372-379. (e) J.-F.Kukowska-Latallo, A. U. Bielinska, J. Johnson, R. Spindler, D. A. Tomalia, J. R. Baker, *Proc. Natl. Acad. Sci. USA* **1996**, *93*, 4897-4902. (f) M. X. Tang, C. T. Redemann, F. C. Szoka, *Bioconjugate Chem.* **1996**, *7*, 703-714. (g) M. An, S. R. Parkin, J. E. DeRouchey, *Soft Matter* **2014**, *10*, 590-599.

4. (a) J.-P. Behr, *Chimia* **1997**, *51*, 34-36. (b) N. D. Sonawane, F. C. Szoka, A. S. Verkman, *J. Biol. Chem.* **2003**, *278*, 44826-44831. (c) Y. Shoji, H. Nakashima, *Curr. Pharm. Des.* **2004**, *10*, 785-796. (d) D. Ouyang, H. Zhang, H. S. Parekh, S. C. Smith, *Biophys. Chem.* **2011**, *158*, 126-133,

5. (a) L. B. Jensen, G. M. Pavan, M. R. Kasimova, S. Rutherford, A. Danani, H. M. Nielsen, C. Foged, *Int. J. Pharm.* **2011**, *416*, 410-418. (b) Y. Tang, Y.-B. Li, B. Wang, R.-Y. Lin, M. van Dongen, D. M. Zurcher, X.-Y. Gu, M. M. B. Holl, G. Liu, R. Qi, *Mol. Pharm.* **2012**, *9*, 1812-1821. (c) S. Biswas, P. P. Deshpande, G. Navarro, N. S. Dodwadkar, V. R. Torchilin, *Biomaterials* **2013**, *34*, 1289-1301. (d) J. Wu, W. Huang, Z. He, *ScientificWorldJournal* **2013**, 630654.

6 (a) M. D. Klein, R. A. Drongowski, R. J. Linhardt, R. S. Langer, *Anal. Biochem.* **1982**, *124*, 59-64. (b) Z. L. Zhong, E. V. Anslyn, *J. Am. Chem. Soc.* **2002**, *124*, 9014-9015. (c) A. T. Wright, Z. L. Zhong, E. V. Anslyn, *Angew. Chem. Int. Ed.* **2005**, *44*, 5679-5682. (d) W. Sun, H. Bandmann, T. Schrader, *Chem. Eur. J.* **2007**, *13*, 7701-7707. (e) M. Wang, D. Q. Zhang, G. X. Zhang, D. B. Zhu, *Chem. Commun.* **2008**, 4469-4471. (f) K. Y. Pu, B. Liu, *Macromolecules* **2008**, *41*, 6636-6640. (g) T. Bříza, Z. Kejík, I. Císařová, J. Králová, P. Martásek, V. Král, *Chem. Commun.* **2008**, 1901-1903. (h) S. L. Wang, Y. T. Chang, *Chem. Commun.* **2008**, 1173-1175. (i) L. T. Zeng, P. F. Wang, H. Y. Zhang, X. Q. Zhuang, Q. Dai, W. M. Liu, *Org. Lett.* **2009**, *11*, 4294-4297. (j) H. Szelke, S. Schübel, J. Harenberg, R. Krämer, *Chem. Commun.* **2010**, *46*, 1667-1669. (k) S. M. Bromfield, A. Barnard, P. Posocco, M. Fermeglia, S. Pricl, D. K. Smith, *J. Am. Chem. Soc.* **2013**, *135*, 2911-2914.

7 (a) W. A. Weiss, J. S. Gilman, A. J. Catenacci, A. E. Osterberg, *J. Am. Med. Assoc.* **1958**, *166*, 603-607. (b) C. W. Lillehei, L. P. Stems, D. M. Long, D. Lepley, *Ann. Surg.* **1960**, *151*, 11-16. (c) T. W. Wakefield, P. C. Andrews, S. K. Wrobleski, A. M. Kadell, A. Fazzalari, B. J. Nichol, T. Van der Kooi, J. C. Stanley, *J. Surgical Res.* **1994**, *56*, 586-593. (d) M. Kikura,

M. K. Lee, J. H. Levy, *Anesth. Analg.* **1996**, *83*, 223-227. (e) S. Choi, D. J. Clements, V. Pophristic, I. Ivanov, S. Vemparala, J. S. Bennett, M. L. Klein, J. D. Winkler, W. F. DeGrado, *Angew. Chem. Int. Ed.* **2005**, *44*, 6685-6689. (f) F. Cunsolo, G. M. L. Consoli, C. Geraci, T. Mecca, *Abiotic Heparin Antagonists,* **2005**, WO/2005/028422. (g) T. Mecca, G. M. L. Consoli, C. Geraci, R. La Spina, F. Cunsolo, *Org. Biomol. Chem.* **2006**, *4*, 3763-3768. (h) M. Schuksz, M. M. Fuster, J. R. Brown, B. E. Crawford, D. P. Ditto, R. Lawrence, C. A. Glass, L. Wang, Y. Tor, J. D. Esko, *Proc. Natl. Acad. Sci. USA* **2008**, *105*, 13075-13080. (i) K. Kaminski, M. Plonka, J. Ciejka, K. Szczubialka, M. Nowakowska, B. Lorkowska, T. Korbut, R. Lach, *J. Med. Chem.* **2011**, *54*, 6586-6596. (j) A. C. Rodrigo, A. Barnard, J. Cooper, D. K. Smith, *Angew. Chem. Int. Ed.* **2011**, *50*, 4675-4679. (k) S. M. Bromfield, P. Posocco, C. W. Chan, M. Calderon, S. E. Guimond, J. E. Turnbull, S. Pricl, D. K. Smith, *Chem. Sci.* **2014**, DOI 10.1039/C4SC00298A

8. S. M. Bromfield, E. Wilde, D. K. Smith, *Chem. Soc. Rev.* **2013**, *42*, 9184-9195.

9. (a) S. Bai, C. Thomas, F. Ahsan, *J. Pharm. Sci.* **2007**, *96*, 2090-2106. (b) B. Klajnert, M. Cangiotti, S. Calici, M. Ionov, J. P. Majoral, A.-M. Caminade, J. Cladera, M. Bryszewska, M. F. Ottaviani, *New J. Chem.* **2009**, *33*, 1087-1093. (c) X. Feng, Y. Cheng, K. Yang, J. Zhang, Q. Wu, T. Xu, *J. Phys. Chem. B* **2010**, *114*, 11017-11026.

10. S. M. Bromfield, P. Posocco, M. Fermeglia, S. Pricl, J. Rodríguez-López,D. K. Smith, *Chem. Comunn.* **2013**, *49*, 4830-4832.

11. (a) J. Zhou, J. Wu, N. Hafdi, J.-P. Behr, P. Erbacher, L. Peng, *Chem. Commun.* **2006**, 2362–2364 (b) X. Liu, P. Rocchi, F. Qu, S. Zheng, Z. Liang, M. Gleave, J. Iovanna, L. Peng, *ChemMedChem* **2009**, *4*, 1302-1310. (c) X. Liu, J. Wu, M. Yammine, J. Zhou, P. Posocco, S. Viel, C. Liu, F. Ziarelli, M. Fermeglia, S. Pricl, G. Victorero, C. Nguyen, P. Erbacher, J.-P. Behr, L. Peng, *Bioconjugate Chem.* **2011**, *22*, 2461-2473. (d) P. Posocco, X. Liu, E. Laurini, D. Marson, C. Chen, C. Liu, M. Fermeglia, P. Rocchi, S. Pricl, L. Peng, *Mol. Pharm.* **2013**, *10*, 3262-3273.

12. (a) H. Yu, Y. Nie, C. Dohmen, Y. Li, E. Wagner, *Biomacromolecules* **2011**, *12*, 2039-2047. (b) W. Cao, L. Zhu, *Macromolecules* **2011**, *44*, 1500-1512. (c) J. Deng, Y. Zhou, B. Xu, K. Mai, Y. Deng, L.-M. Zhang, *Biomacromolecules* **2011**, *12*, 642-649. (d) J. Deng, N. Li, K. Ma, C. Yang, L. Yan, L.-M. Zhang, *J. Mater. Chem.* **2011**, *21*, 5273-5281. (e) T. Tanaka, K. Shibata, M. Hosokawa, K. Hatakeyama, A. Arakaki, H. Gomyo, T. Mogi, T. Taguchi, H. Wake, T. Tanaami, T. Matsunami, *J. Colloid Interface Sci.* **2012**, *377*, 469-475. (f) B. Liang, J. J. Deng, F. Yuan, N. Yang, W. Li, J. T. Yin, S. X. Pu, L. C. Sie, C. Gao, L. M. Zhang, *Carbohydrate Polym.* **2013**, *94*, 185-192.

13. (a) J. Zhou, J. Wu, X. Liu, F. Qu, M. Xiao, Y. Zhang, L. Charles, C.-C. Zhang, L. Peng, *Org. Biomol. Chem.* **2006**, *4*, 581-585. (b) T. Yu, X. Liu, A.-L. Bolcato-Bellemin, Y. Wang, C. Liu, P. Erbacher, F. Qu, P. Rocchi, J.-P. Behr, L. Peng, *Angew. Chem. Int. Ed.* **2012**, *51*, 8478-8484. (c) K. Kono, R. Ikeda, K. Tsukamoto, E. Yuba, C. Kojima, A. Harada, *Bioconjugate Chem.* **2012**, *23*, 871-879. (d) S. Iwashita, Y. Hiramatsu, T. Otani, C. Amano, M. Hirai, K. Oie, E. Yuba, K. Kono, M. Miyamoto, K. Igarashi, *J. Biomater. Appl.* **2012**, *27*, 445-456. (e) Y. Zhang, J. Chen, C. Xiao, M. Li, H. Tian, X. Chen, *Biomacromolecules* **2013**, *14*, 4289-4300.

14. (a) A. C. Rodrigo, I. Rivilla, F. C. Pérez-Martínez, S. Monteagudo, V. Ocaña, J. Guerra, J. C. García-Martínez, S. Merino, P. Sánchez-Verdú, V. Ceña, J. Rodríguez-López, *Biomacromolecules* **2011**, *12*, 1205-1213. (b) G. M. Pavan, S. Monteagudo, J. Guerra, B. Carrión, V. Ocaña, F. J. Rodríguez, A. Danani, F. C. Perez-Martinez, V. Ceña, V. *Curr. Med. Chem.* **2012**, *19*, 4929-4941. (c) M., D. Pérez-Carrión, V. Ceña, *Pharm. Res.* **2013**, *30*, 2584-2595.

15 G. M. Pavan, A. Danani, *Phys. Chem. Chem. Phys.* **2010**, *12*, 13914-13917.

16. (a) P. K. Maiti, T. Cagin, S.-T. Lin, W. A. Goddard III, *Macromolecules* **2005**, *38*, 979-991; (b) Y. Liu, V. S. Bryantsev, M. S. Diallo, W. A. Goddard III, *J. Am. Chem. Soc.* **2009**, *131*, 2798-2799.

17. G. M. Pavan, A. Danani, S. Pricl, D. K. Smith, *J. Am. Chem. Soc.* **2009**, *131*, 9686-9694.

18. H Szelke, S. Schübel, J. Harenberg, R. Krämer, *Bioorg. Med. Chem. Lett.,* **2010**, *20*, 1445-1447

19. (a) M. O. Steinhauser, *Computational Mutiscale Modeling of Fluids and Solids – Theory and Applications,* Springer-Verlag, Heidelberg, **2008**. (b) P. Posocco, S. Pricl, S. P. Jones, A. Barnard, D. K. Smith, *Chem. Sci.* **2010**, *1*, 393-404. (c) A. Barnard, P. Posocco, S. Pricl, M. Calderon, R. Haag, M. E. Hwang, V. W. T. Shum, D. W. Pack, D. K. Smith, *J. Am. Chem. Soc.* **2011**, *133*, 20288-20300; (d) S. P. Jones, N. P. Gabrielson, C.-H. Wong, H.-F. Chow, D. W. Pack, P. Posocco, M. Fermeglia, S. Pricl, D. K. Smith, *Mol. Pharm.* **2011**, *8*, 416-429. (e) P. Posocco, E. Laurini, V. Dal Col, D. Marson, L. Peng, D. K. Smith, B. Klajnert, M. Bryszewska, A.-M. Caminade, J.-P. Majoral, M. Fermeglia, K. Karatasos, S. Pricl In *Dendrimers in Biomedical Applications*, B. Klajnert, L. Peng, V. Ceña, Eds., RSC Publishing: Cambridge **2013**, pp 148-166; (f) P. Posocco, E. Laurini, V. Dal Col, D. Marson, K. Karatasos, M. Fermeglia, S. Pricl, *Curr. Med. Chem.* **2012**, *19*, 5062-5087; (g) D. J. Welsh, P. Posocco, S. Pricl, D. K. Smith, *Org. Biomol. Chem.* **2013**, *11*, 3177-3186 (h) A. Barnard, P. Posocco, M. Fermeglia, A. Tschiche, M. Calderon, S. Pricl, D. K. Smith, *Org. Biomol. Chem.* **2014**, *12*, 446-455.

20. For the software see: (a) D. A. Case, T. A. Darden, T. E. Cheatham III, C. L. Simmerling, J. Wang, R. E. Duke, R. Luo, R. C. Walker, W. Zhang, K. M. Merz, B. Roberts, B. Wang, S. Hayik, A. Roitberg, G. Seabra, I. Kolossváry, K. F. Wong, F. Paesani, J. Vanicek, X. Wu, S. R. Brozell, T. Steinbrecher, H. Gohlke, Q. Cai, X. Ye, J. Wang, M.-J. Hsieh, G. Cui, D. R. Roe, D. H. Mathews, M. G. Seetin, C. Sagui, V. Babin, T. Luchko, S. Gusarov, A. Kovalenko and P. A. Kollman AMBER 11, **2010**, University of California, San Francisco, CA, USA. For key papers: (b) W. L. Jorgensen, J. Chandrasekhar, J. D. Madura, R. W. Impey, M. L. Klein, *J. Chem. Phys.* **1983**, *79*, 926-935. (c) A. Toukmaji, C. Sagui, J. Board, T. Darden, *J. Chem. Phys.* **2000**, *113*, 10913-10927. (d) J. Wang, R. M. Wolf, J. Caldwell, P. A. Kollman, D. A. Case, *J. Comput. Chem.* **2004**, *25*, 1157-1174. (e) J. Wang, P. A. Kollman, D. A. Case, *J. Mol. Graph. Model.* **2006**, *25*, 247-260. (f) S. P. Jones, G. M. Pavan, A. Danani, S. Pricl, F. K. Smith, *Chem. Eur. J.* **2010**, *16*, 4519-4532. (g) G. M. Pavan, P. Posocco, A. Tagliabue, M. Maly, A. Malek, A. Danani, E. Ragg, C. V. Catapano, S. Pricl, *Chem. Eur. J.* **2010**, *16*, 7781-7795.

21. (a) G. M. Pavan, L. Albertazzi, A. Danani, *J. Phys. Chem. B* **2010**, *114*, 2667-2675. (b) C. Sun, T. Tang, H. Uludag, *J. Phts. Chem. B* **2012**, *116*, 2405-2413.

22. (a) P. J. Hoogerbrugge, J. M. V. A. Koelman, *Europhys. Lett.* **1992**, *19*, 155-160. (b) R. D. Groot, P. B. Warren, P. B. *J. Chem. Phys.* **1997**, *107*, 4423-4435.

23 C. Sun, T. T'ang, H. Uludag, *Biomacromolecules* **2011**, *12*, 3698-3707.

24. Transgedens with alcohol surface groups Compound G1-$(OH)_9$ has not been described so far. ^{1}H-NMR (500 MHz, CD_3OD) δ: 2.34 (t, 12H, J = 6.5 Hz, 6×CH_2), 2.44 (t, 6H, J = 6.5 Hz, 3×CH_2), 2.61 (broad s, 12H, 6×CH_2), 2.73 (t, 12H, J = 6.5 Hz, 6×CH_2), 2.83 (t, 6H, J = 6.5 Hz, 3×CH_2), 3.28 (t, 12H, J = 6.5 Hz, 6×CH_2), 3.30-3.36 (m, 6H), 3.58 (t, 12H, J = 6.5 Hz, 6×CH_2), 3.63 (t, 6H, J = 6.5 Hz, 3×CH_2), 3.65 (s, 6H, 3×CH_2Ar), 7.20 (A of AB_q, 3H, J = 16.0 Hz, 3×CH=), 7.28 (B of AB_q, 3H, J = 16.0 Hz, 3CH=), 7.35 (A of AB_q, 6H, J = 8.0 Hz, ArH), 7.56 (B of AB_q, 6H, J = 8.0 Hz, ArH), 7.62 (s, 3H, ArH). ^{13}C NMR and DEPT (125 MHz, CD_3OD) δ: 175.4 (CO), 175.2 (CO), 139.9 (C), 139.7 (C), 137.8 (C), 130.7 (CH), 130.1 (CH), 129.3 (CH), 127.7 (CH), 124.9 (CH), 61.7 (CH_2), 61.6 (CH_2), 59.7 (CH_2), 52.4 (CH_2), 52.3 (CH_2), 51.7 (CH_2), 51.2 (CH_2), 42.9 (CH_2), 34.5 (CH_2), 34.4 (CH_2). IR (ATR) ν**:** 3278 (broad), 2929, 2818, 1633, 1548, 1059 cm^{-1}. MALDI-TOF (THAP) m/z: 1637.6 $[M+H]^+$.

25. J. Guerra, A. C. Rodrigo, S. Merino, J. Tejeda, J. C. García-Martínez, P. Sánchez-Verdú, V. Ceña, J. Rodríguez-López, *Macromolecules* **2013**, *46*, 7316-7324.

26. C. L. Gettinger, A. J. Heeger, J. M. Drake, D. J. Pine, *J. Chem. Phys.* **1994**, *101*, 1673-1678.

Received: ((will be filled in by the editorial staff))
Revised: ((will be filled in by the editorial staff))
Published online: ((will be filled in by the editorial staff))

DOI: 10.1002/chem.201xxxxxx

Entry for the Table of Contents

FULL PAPER

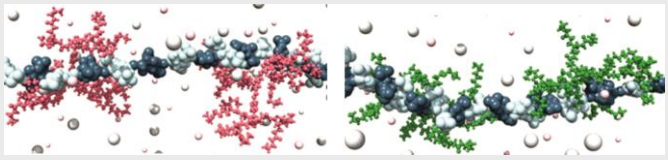

The inside of the dendrimer controls the display of the surface ligands – rigid TGDs (shown in red) have locally organised shape-persistent multivalent surface groups which can only bind well if several different heparin chains are present to satisfy all the rigidly displayed surface groups, while PAMAMs (shown in green) have flexible structures which show adaptive multivalency to wrap around a single heparin chain.

Supramolecular Nanoscience

Stephen M. Bromfield, Paola Posocco, Maurizio Fermeglia, Juan Tolosa, Ana Herreros-López, Sabrina Pricl, Julián Rodríguez-López* and David K. Smith**

■■ – ■■

Shape-Persistent and Adaptive Multivalency – Rigid Transgeden (TGD) and Flexible PAMAM Dendrimers for Heparin Binding